Research Article

Mahendra, I.P., Wirjosentono, B.*, Tamrin, Ismail, H., Mendez, J.A.

Thermal and Morphology Properties of Cellulose Nanofiber from TEMPO-oxidized Lower part of Empty Fruit Bunches (LEFB)

https://doi.org/10.1515/chem-2019-0063
received August 14, 2018; accepted March 19, 2019.

Abstract: Cellulose nanofiber (CNF) gel has been obtained from TEMPO-oxidized differently treated lower part of empty fruit bunches (LEFB) of oil palm. Three kinds of materials were initially used: (i) α-cellulose, (ii) raw LEFB fiber two-times bleaching, and (iii) raw LEFB three-times bleaching. The obtained nanofibers (CNF1, CNF2 and CNF3, respectively) were then characterized using several methods, e.g. FT-IR, SEM, UV-Visible, TEM, XRD and TGA. The LEFB at different levels of bleaching showed that the Kappa number decreased with the increase of the bleaching levels. The decrease of lignin and hemicellulose content affected the increase of the yield of fibrillation and optical transmittance of CNF2 and CNF3 gels. The FT-IR analysis confirmed the presence of lignin and hemicellulose in the CNF2 and CNF3 film. Based on TEM analysis, the lignin and hemicellulose content significantly affected the particle structure of CNFs, *i.e.* CNF1 was found as a bundle of fibril, while the CNF2 and CNF3 were visualized as individual fibers and interwoven nanofibril overlapping each other, respectively. The XRD data of the CNF's film showed that CNF2 and CNF3 have a lower crystallinity index (CI) than CNF1. The presence of lignin and hemicellulose in the CNFs decreased its decomposition temperature.

***Corresponding author: Wirjosentono, B.,** Departemen Kimia, Fakultas Matematika dan Ilmu Pengetahuan Alam, Universitas Sumatera Utara, Medan, Indonesia, E-mail: basuki@usu.ac.id
Mahendra, I.P., Tamrin: Departemen Kimia, Fakultas Matematika dan Ilmu Pengetahuan Alam, Universitas Sumatera Utara, Medan, Indonesia
Ismail, H.: School of Material and Mineral Resources Eng. Universiti Sains Malaysia, Penang, Malaysia
Mendez, J.A.: Enginyeria Química, Agrària i Tecnologia Agroalimentària, Universitat de Girona, Politècnica I, Campus Montilivi, Girona, Spain

Keywords: TEMPO; Cellulose Nanofiber; Bleaching level; Empty Fruit Bunch; Oil Palm.

1 Introduction

As one of the largest palm oil exporters and producers, Indonesia has 11.12 million hectares of land that cultivates the oil palm, which produced 31 million tons of CPO, in 2016; and which also produced 125.46 million tons waste of the empty fruit bunch (EFB) [1]. The lower part of the empty fruit bunch (LEFB) oil palm can be categorized as lignocellulosic waste, which consists of cellulose, hemicellulose, lignin, extractive components and ash (Table 1). The high content of cellulose in this lignocellulosic waste can be utilized as raw material for CNF production.

CNF has wide areas of application due to its interesting properties, such as low weight, high aspect ratio, high reinforcing potential, and large surface area [2,3]. CNF can also be applied in a variety of industrial areas or applications, such as nanofiller for polymeric nanocomposite, packaging and food packaging, paper printing, antibacterial paper, and conductive paper [3–7].

The separation of CNF from the cellulose fibers is problematic because the fibers are connected to one another via hydrogen bonds and van der Waals interactions. Several methods can be used to separate CNF from the cellulose fiber, such as chemical, mechanical and chemo-mechanical treatments. For the chemical treatment, sulphuric acid hydrolysis was used to obtain cellulose nanofiber from the EFB with the yield of fibrillation around 30% [8]. The acid hydrolysis method was combined with a high pressure homogenizer to obtain the homogenous size of nanofiber from the microfibril cellulose fiber [9]. Ultrasonication using oscillating power was a mechanical approach to obtaining nanosized fiber from isolated micro-size cellulose fiber.

Open Access. © 2019 Mahendra, I.P. et al., published by De Gruyter. This work is licensed under the Creative Commons Attribution alone 4.0 License.

Brought to you by | Universitat de Girona
Authenticated
Download Date | 1/31/20 2:37 PM

Table 1: The oil palm fiber's composition (wt.%) [20].

Part	Cellulose	Hemicellulose	Lignin		Extractive	Ash
			Klason	Acid Soluble		
Trunk	30.6	33.2	24.7	3.8	3.6	4.1
EFB	37.9	35.0	22.9	1.1	2.7	1.5

In the past decade, CNF with individual nanofibril was successfully obtained using 2,2,6,6-tetramethyl-1-piperidinyloxyl (TEMPO) catalytic oxidation treatment with the addition of NaClO and NaBr (pH 10) [10,11]. TEMPO catalytic oxidation was used to obtain cellulose nanofibril with the various kinds of cellulosic materials, such as eucalyptus pulp [12], *N. oceanica* microalgae [13], commercial microcrystalline [14], bacterial cellulose [15], and various plant holocelluloses [16]. However, to date, no studies have been found on the preparation of CNF from the LEFB raw fiber and LEFB α-cellulose through TEMPO catalytic oxidation. The previous studies focused on the isolation of nanocrystalline cellulose [17] and CNF from EFB were prepared using H_2SO_4 hydrolysis; the thickness of obtained fiber ranged from 1-3.5 nm [18].

The characteristics of CNF, especially the morphology and thermal properties, depend on the source of starting materials (fiber) and precise treatment conditions (concentration, temperature, and reaction time). However, past studies had focused on the effects of different bleaching level towards the characteristics of the obtained fiber. The bleaching treatment has been identified as an important parameter to be considered during the preparation of nanocellulose [19]. Therefore, this research was focused on the thermal and morphology properties of CNFs that were prepared from several differently treated LEFBs, especially where the level of LEFB bleaching was concerned. The isolation of CNF was performed using α-cellulose and raw LEFB fiber. Specifically, the raw fiber of LEFB was treated by removing lignin and hemicellulose during the bleaching treatment. In the end, α-cellulose and the bleached LEFB were oxidized using TEMPO and passed through the high-pressure homogenizer to improve the possibility of obtaining nanosized fiber. This study aims to utilize LEFB fiber, an abundant renewable source as a raw material for the production of CNF using the TEMPO method that combines high pressure homogenization as a chemo-mechanical treatment. This study will open up new avenues for the effective utilization of the underutilized resources for the preparation of nanoscale materials. In addition, the FT-IR, SEM, TEM, XRD and TGA were employed to evaluate the properties of CNF.

2 Experimental Method

2.1 Materials

LEFB was obtained from a oil palm plantation in Riau, Indonesia. Hydrogen peroxide (50 wt.%), 2,2,6,6-tetramethyl-1-piperidinyloxyl (TEMPO), sodium hypochlorite and sodium bromide were purchased from Sigma Aldrich. Nitric acid (70 wt.%), sodium nitrite, sodium hydroxide, and sodium sulfite were purchased form Merck. All chemicals were used without additional treatment.

2.2 Method A

2.2.1 Preparation of the LEFB fiber

The lower part of the empty fruit bunch (LEFB) was chopped to a dimension of 1 cm x 1 cm. The lower part of the LEFB was then dried at 80°C for 48 h and ground to a fine powder (the powder was sieved through 200 μm particle size).

2.2.2 Preparation of α-cellulose

The isolation of cellulose followed the modified method that was described by Ohwoavworhua et al. [21]. About 75 g of the LEFB was weighed then soaked with 1 L of 3,5 wt.% HNO_3 and 10 mg of $NaNO_2$ at 90°C for 2 hours. The neutralized fibers reacted with 750 mL of 2 wt.% NaOH and Na_2SO_3 at 50°C for 1 h. The obtained fibers were neutralized using distillate water and bleached with 250 mL of 1,75 wt.% NaClO. The fibers were washed using distillated water, and the filtrated water was tested by $AgNO_3$ to verify that it was free of chloride ions. After this which was to remove the hemicellulose components, the powder was soaked in 1,75 wt.% NaOH at 80°C and washed until it reached a pH of 7. The residue was then bleached using 10 wt.% H_2O_2 at 60°C for 15 minutes and washed until the pH was neutral.

Brought to you by | Universitat de Girona
Authenticated
Download Date | 1/31/20 2:37 PM

2.2.3 Preparation of Nano Fibrillated Cellulose (CNF)

The TEMPO oxidized CNF was prepared from α-cellulose by following the method that is described by Saito et al. [11]. The TEMPO and NaBr with the amount of 0.016 and 0.1 g/g of fiber were added respectively into the dispersion of α-cellulose with a consistency of 1%. After a good dispersion was obtained, 7.2 wt.% of NaClO was added to the slurry until the concentration of NaClO reached 10 mmol/ g of cellulose. The TEMPO reaction was maintained at pH 10 for 5 h by the addition of NaOH 0.5 N. Then, the oxidized α-cellulose was thoroughly filtrated and washed three times. The mixture was homogenized at 8000 rpm, then continued with ultrasonication for 4 minutes. This cellulose product was coded as CNF1.

2.3 Method B

2.3.1 Fiber Conditioning

The LEFB fiber was chopped using knives mill from Agrimsa (St. Adria` del Beso's, Spain) provided with a 10 mm mesh. 100 g of fiber was subjected to the bleaching process using 10 wt.% of H_2O_2 (1:10); the pH was kept at 10 by adding dropwise NaOH 4 N. Then the mixture was stirred at 1000 rpm for 2 h at room temperature. The neutral bleach was rinsed with water and passed to the Sprout-Waldron defibrator (model 105-A) to increase the fiber individualization. The obtained fiber was filtered and and measured for moisture content. Fiber (10 wt.% of dry weight) was milled in a PFI mill (NPFI 02 Metrosec S.A) at 4000 revolutions. The milled fiber was dispersed in solution of 1 wt.% of H_2O_2 (1:10) and the pH was adjusted to 10 by adding dropwise NaOH 4 N. The mixture was stirred at 1000 rpm for 2 h at room temperature. The second bleached fiber was then dispersed in 5 wt.% of H_2O_2 (1:10) and the pH was adjusted to 10 by adding dropwise NaOH 4 N. The mixture was stirred at 1000 rpm and 60°C of temperature for 2 h. The bleached product was filtrated and washed until a neutral pH was obtained and stored at 15°C.

2.3.2 Preparation of Nano fibrillated Cellulose / Lignocellulose

The bleached LEFB fiber was pre-treated with TEMPO/ NaClO/ NaBr according to the previous steps (2.2.3. CNF oxidized TEMPO of α-cellulose). The oxidized LEFB was washed three times. According to the bleaching level, the CNF was coded as CNF2 (second bleaching) and CNF3 (third bleaching). The carboxyl content and cationic demand of CNF2 and CNF3 were 985 μmol/g and 1.238,8 μeq/g, respectively. Those values confirmed the presence of carboxylic group as the result of TEMPO oxidation reaction.

2.4 Fibrillation Process

The fibrillation process was performed using a high-pressure homogenizer (NS1001L PANDA 2K-GEA) by passing 1 wt.% fiber suspension. The operational conditions were set to 600 bars of pressure and the fiber was passed through the machine six times. The obtained transparent gel-like suspension was preserved at 4°C.

2.5 Characterization

2.5.1 Kappa Number

Kappa number, which is a measure of the lignin content of the fiber was determined by the titration method in accordance with TAPPI standard T-236 cm-85.

2.5.2 Optical Transmittance and Yield of Fibrillation

The transmittance of the CNF suspension (0.1 wt.%) was determined at 400-800 nm using a UV-Vis Spechtrophotometer 160A (Shimadzu). The yield of fibrillation was determined after the centrifugation process of 100 mL of the CNF suspension (0.1 wt.%) at 4.500 rpm for 20 min. The yield fibrillation was calculated using the equation below:

$$Yield\ (\%) = \left(1 - \frac{weight\ of\ dried\ fiber}{weight\ of\ diluted\ sample\ x\ \%Sc}\right) x100\% \qquad (1)$$

where %Sc refers to the solid content of the diluted fiber.

2.5.3 FT-IR analysis

The spectra of α-cellulose powder and all CNF's film were recorded on the FT-IR spectrophotometer 8201PC Shimadzu. The sample was pulverized and mixed with KBr with composition of sample 1 mg/100 mg. The sample was scanned 64 times, with the spectra transmittance region between a wavenumber 4000 to 500cm^{-1} at 4 cm^{-1} of resolution.

Brought to you by | Universitat de Girona
Authenticated
Download Date | 1/31/20 2:37 PM

2.5.4 XRD analysis

The XRD experiment was performed using XRD Shimadzu 6100 X-ray diffractometers. The α-cellulose powder and all CNF's film were scanned in the reflection mode using an incident X-ray of CuKα with a wavelength of 1.54 Å at a step width of 0.05 ° min^{-1} from 2θ = 0-80°. The crystallinity index (CrI) was defined by Segal [22] Eq. (2):

$$CrI(\%) = \frac{I_{002} - I_{100}}{I_{002}} x100 \quad (2)$$

where I_{002} and I_{100} were the intensity peak for the crystalline cellulose and amorphous cellulose, respectively.

2.5.5 Surface morphological characterization

The surface morphological characterization of α-cellulose powder and all CNF's gel were carried out under a scanning electron microscope (SEM) using ZEISS EVO MA 10. The α-cellulose was gold-sputtered using a sputter coater. The transparent gel-like suspension of CNF was placed on the sample holder. After being dried, all CNFs were gold-sputtered using a sputter coater to enhance the conductivity of the sample.

2.5.6 TEM analysis

The structural dimensions of all CNF's gel were observed by TEM JEOL JEM 1400 with an accelerated voltage of 80 kV. The sample was dissolved in water to obtain a suspension. A drop of suspension was placed on copper grids coated with a carbon supported film; the solvent evaporated.

2.5.7 Thermal Analysis (TGA)

The thermal stability of α-cellulose powder and all CNF's film was examined by thermogravimetric analysis (TGA) using TG/DTA STA 7300 with the range of temperature of 30-600°C (2°C/min). The heating process was carried out under a nitrogen atmosphere to prevent any thermoxidative degradation. The residual mass at 600°C was directly obtained from the measurement data.

2.5.8 Ethical Approval

The conducted research is not related to either human or animal use.

3 Result and Discussion

α-cellulose was successfully isolated from cleaned and dried LEFB through a straightforward two-step process, such as the delignification and hemicellulose removing process. The LEFB powder color turned white after delignification and hemicellulose removal. After confirmation through FT-IR analysis (Figure 1), the obtained white powder was identified as α-cellulose. In the spectrum of isolated α-cellulose form the LEFB, it had a similar band with the reference of α-cellulose but different in intensity.

The FT-IR spectra of all CNFs that were prepared from LEFB is shown in Figure 1. The presence of ν(O-H) stretching and ν(CH_3)/ ν(CH) groups in the FT-IR spectra of all CNFs are shown as signals around 3300-3600 and 2800-2900 cm^{-1}, respectively. The presence of a carboxylic group can be confirmed from a specific band at 1650 cm^{-1}. It indicates that absorbed water was present by the result of carboxylate group interaction. The presence of lignin can be confirmed by the presence of a band around 1510-1400 cm^{-1}. This result is in line with the result of Ahuja et al. [23]. The raw fiber, after chemical treatment, will have a significant difference in FT-IR spectra, especially around 1510 and 1420 cm^{-1}. The significant decrease of those areas is considered to be the partial removal of lignin.

The oxidation of the hydroxyl group at C6 of cellulose mediated by TEMPO (Figure 2), was done solely for this position. The oxidation reaction mechanism of cellulose through the TEMPO oxidation was relatively selective, simple and efficient. The oxidation process using TEMPO was combined with the presence of NaClO/NaBr or NaClO/$NaClO_2$ as the primary oxidants, and the

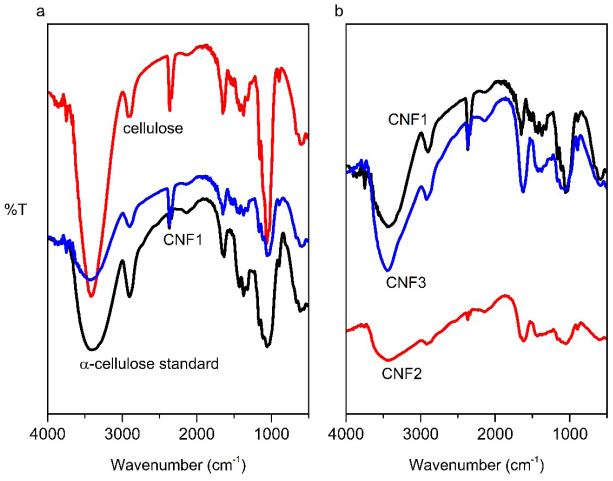

Figure 1: FT-IR spectra of α-cellulose and all CNF products.

Brought to you by | Universitat de Girona
Authenticated
Download Date | 1/31/20 2:37 PM

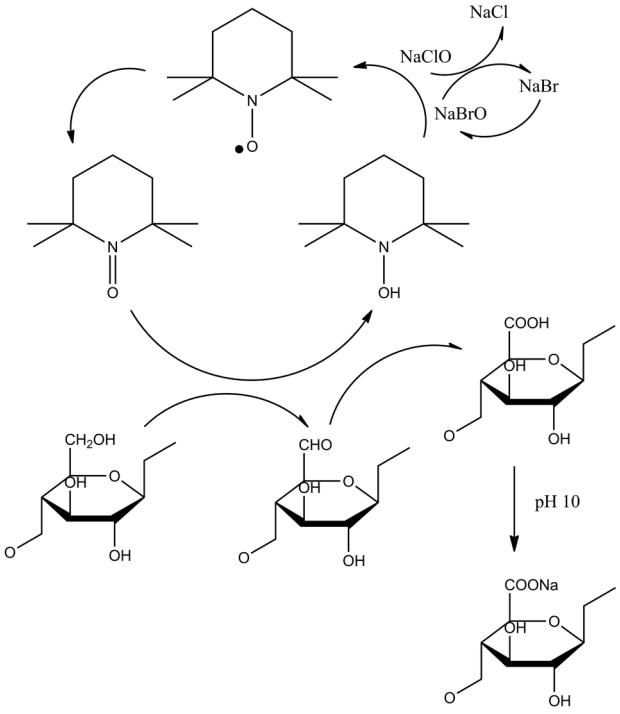

Figure 2: Pathway of oxidation process of C6 primary hydroxyl to carboxylate group [24].

reaction could be performed within a wide range of pH, notably pH 4-10 [16,24–28]. Before the TEMPO-oxidized treatment, in method B, the fiber was processed with mechanical treatments using Sprout-Waldron and PFI-mill. These mechanical treatments facilitated the TEMPO-oxidized fiber to pass through the homogenizer and to allow the fiber to have a greater capacity for hydration and swelling. Without these mechanical treatments, the TEMPO-oxidized fiber could not have passed through the homogenizer because of the significant difference in fiber size. As a result, the nanosized particle of the CNF can be seen in Figure 3 and Figure 5.

The morphology of the isolated α-cellulose and CNF is shown in Figure 3. The morphology of α-cellulose powder (Figure 3a) showed curled and well-defined fibrils as the impact of interfibrillar hydrogen bonding of the hydroxyl group on the fibril surface. The isolated α-cellulose fibers have an average diameter of 27.3 ± 7.4 μm.

The observation of the dried transparent gel-like suspension of CNFs revealed that the width of the fibril was in the range of 10-130 nm (Figure 3b-d). The interwoven nanofibril overlapping each other was only observed in the CNF3. This result shows evidence of the potential of CNF to be a good nanofiller when it is incorporated with the polymer matrix through an entanglement mechanism.

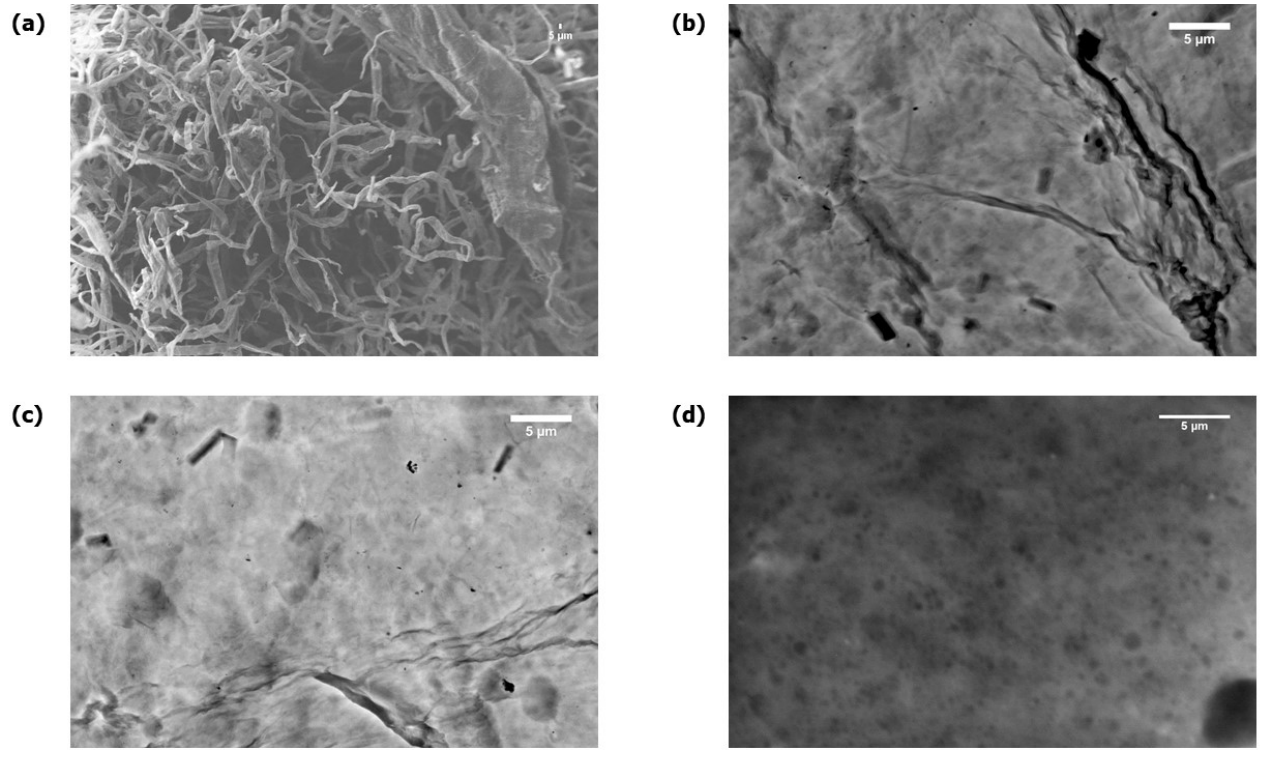

Figure 3: The SEM images of (a) α-cellulose, (b) CNF1, (c) CNF2 and (d) CNF3.

Brought to you by | Universitat de Girona
Authenticated
Download Date | 1/31/20 2:37 PM

Table 2: Characteristic of CNF from LEFB.

Code	Kappa Number	Yield of Fibrillation (%)
CNF1	Not measured	76.00
CNF2	9.3	78.11
CNF3	3.8	90.00

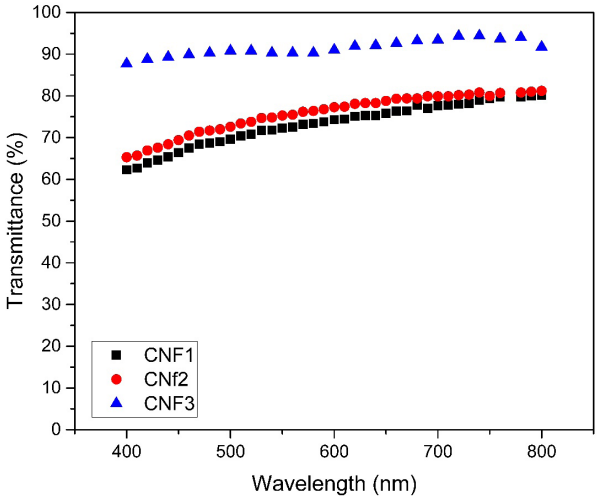

Figure 4: UV-Vis transmittance spectra of CNF.

The interwoven fibril was not observed in the CNF1 and CNF2 samples, but from these fibers, a bundle of fibril formed aggregates. The aggregates confirm that the nanofibril resulted from the physical break-up of the aggregated microfibril [29].

The Kappa number of the bleached fiber decreased inversely with the increase of the bleaching treatment (Table 2). The Kappa number is used to determine the amount of lignin in the fiber sample; in other words the Kappa number shows a direct relationship with the lignin content of the fiber. The combination effect between hydrogen peroxide and sodium hydroxide during the bleaching process at 60°C seemed to remove the hemicellulose and lignin content significantly; with this treatment a higher content of cellulose could be obtained [30]. The content of hemicelluloses in the fiber was controlled through bleaching treatment that was supported under alkaline conditions [31]. The results of the Kappa number supported the FT-IR spectra (Figure 1), and that the lignin in the treated fiber was partially removed.

An additional effect of the level of bleaching is shown through the yield of the fibrillation value. The increase of the bleaching treatment in CNF2 and CNF3 has a positive impact to the increase of the yield fibrillation. The yield of fibrillation is dependent on the reduction of the Kappa number or lignin content [31,32]. This relationship can be determined by using an indirect method of measuring the transmittance of CNF suspension (Figure 4).

The suspension with a lower fibrillated CNF will scatter more light than the suspension with a higher yield of fibrillation. The third bleached fiber (CNF3) has a lower Kappa number (3.8) than the second bleached fiber (9.3) (CNF2). It showed the third bleached fiber had a slightly higher light transmittance and yield of fibrillation than the second bleached fiber. These results were relatively close when compared to the CNF obtained from the eucalyptus fiber that was processed with TEMPO/NaClO/NaBr [12,32]. The content of lignin also influenced the properties of the TEMPO-oxidized nanofiber. The presence of lignin during the TEMPO-oxidized reaction caused the fiber not to be perfectly oxidized by TEMPO/ NaClO/ NaBr, because some parts of the oxidant reacted with the lignin in the fiber to promote the delignification process. This is shown by the dark color of the solution during the oxidation reaction. CNF1 had a lower value of the yield of fibrillation, and it can be assumed it was due to an impact of the low content of hemicellulose [31]. The optical transmittance measurement can be used to evaluate the opacity of the obtained CNF fiber as well. The CNF3 is optically transparent, which showed a 90% light transmittance at a wavelength above 500 nm. On the other hand, CNF1 and CNF2 had relatively low light transmittance compared to CNF3, about 70% light transmittance at a wavelength above 500 nm. CNF1 and CNF2 exhibit a transmittance of 80% at a wavelength of 790 and 660 nm, respectively. The material which has more than 80% light transmittance is considered transparent [33].

TEM analysis was performed to obtain the accurate data about the widths of all prepared CNFs. From the TEM observation shown in Figure 5, the morphology of CNF from CNF1, CNF2 and CNF3 obtained with and without high pressure homogenization is quite different. All prepared CNFs showed that the diameter of CNF has a nanosized scale with a width ranging from 3 to 50 nm and several microns of length.

Figure 5a shows the shape of the CNF1 fiber, forming a bundle of microfibrils with the dimensions of 324 and 167 nm of length and width, respectively. This phenomenon occurred due to the low content of hemicellulose, where as stated by Chaker et al, hemicellulose content was found to have an influence towards the aggregation of fibers [31]. The high content of hemicellulose in the fiber made the fiber stays apart as an individual fiber. Figures 5b and 5c, show the obtained fiber CNF2 and CNF3 respectively. They have different appearances compared to CNF1. The

Brought to you by | Universitat de Girona
Authenticated
Download Date | 1/31/20 2:37 PM

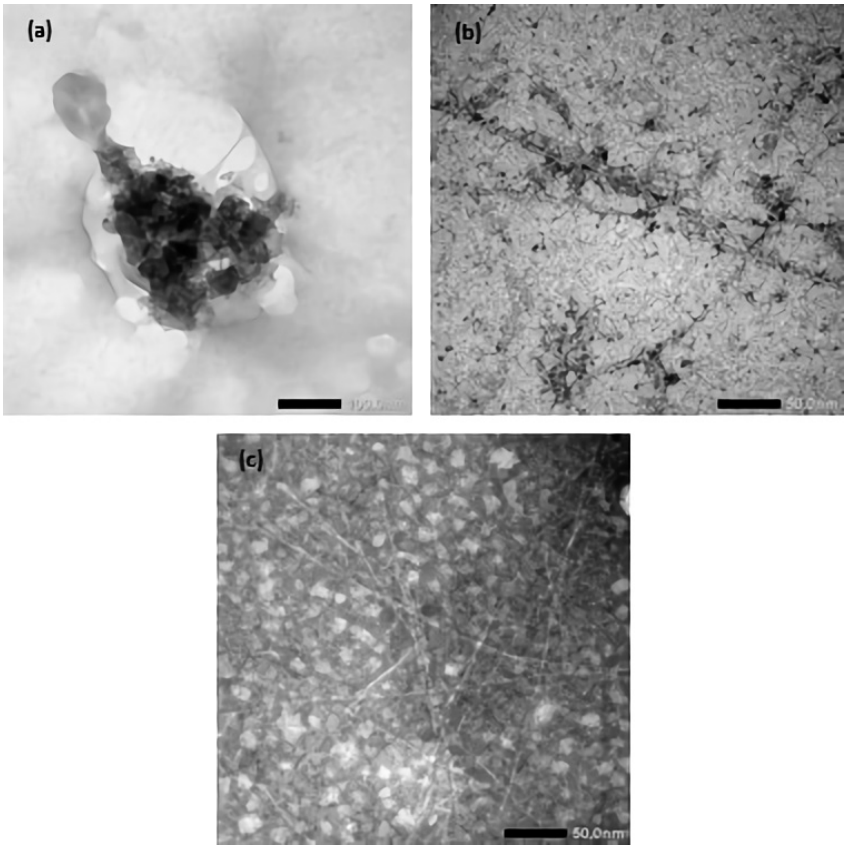

Figure 5: TEM images of all CNF (a) CNF1, (b) CNF2 and (c) CNF3.

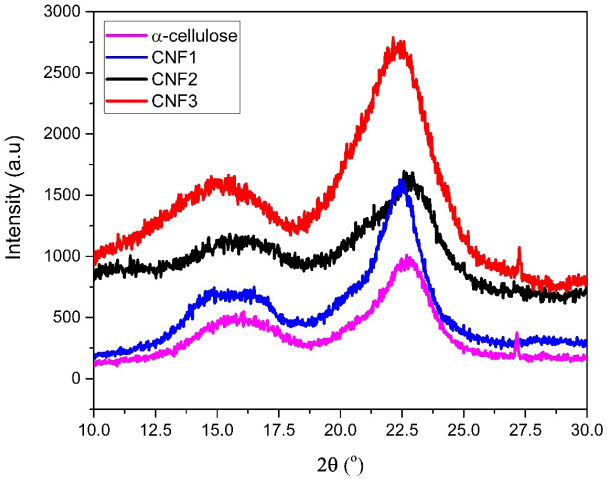

Figure 6: XRD spectra of α-cellulose and CNFs.

CNF2 fiber is more individualized than CNF1 and CNF3. This is the impact of CNF2 having a higher content of hemicellulose than CNF3. The CNF3 has a high potential to lose the hemicellulose content than CNF2 because of the higher number of bleaching treatments on CNF3 compared to CNF2. A thin web like fiber was observed in CNF3. The fiber formed a highly interwoven microfibril overlapping each other. This formation could improve the potential of CNF3 as a nanofiller when utilized in a polymer matrix, as it has a higher value of aspect ratio than CNF2, i.e 265.19 (CNF3) and 229.09 (CNF2).

The XRD patterns of the α-cellulose powder and CNFs from LEFB are shown in Figure 6. The presence of the crystalline region is not only represented by the diffraction peak at 2θ = 22.5° but also 14.8 and 16.5° which points to the 1$\bar{1}$0 and 110 lattice planes of cellulose [34,35]. In Figure 6, both the peaks at 14.8 and 16.5° are not observed, as the presence of those peaks depends on the source of the fiber [35]. The crystallinity index (CI) of α-cellulose is slightly higher than the CNF1, CNF2 and CNF3 which were 73,69; 73,45; 43,61 and 55,26%, respectively. The lower value of the crystallinity index after the TEMPO oxidation reaction and fibrillation treatment was also supported by Rohaizu and Wanrosli [34] and Besbes et al. [29]. The lower value of CNF2 and CNF3 than the α-cellulose could be caused by the presence of lignin and hemicellulose. The crystallinity index between CNF2 and CNF3 is influenced by the number of bleaching level, in which NF3 has a higher value of crystallinity index than CNF2.

Brought to you by | Universitat de Girona
Authenticated
Download Date | 1/31/20 2:37 PM

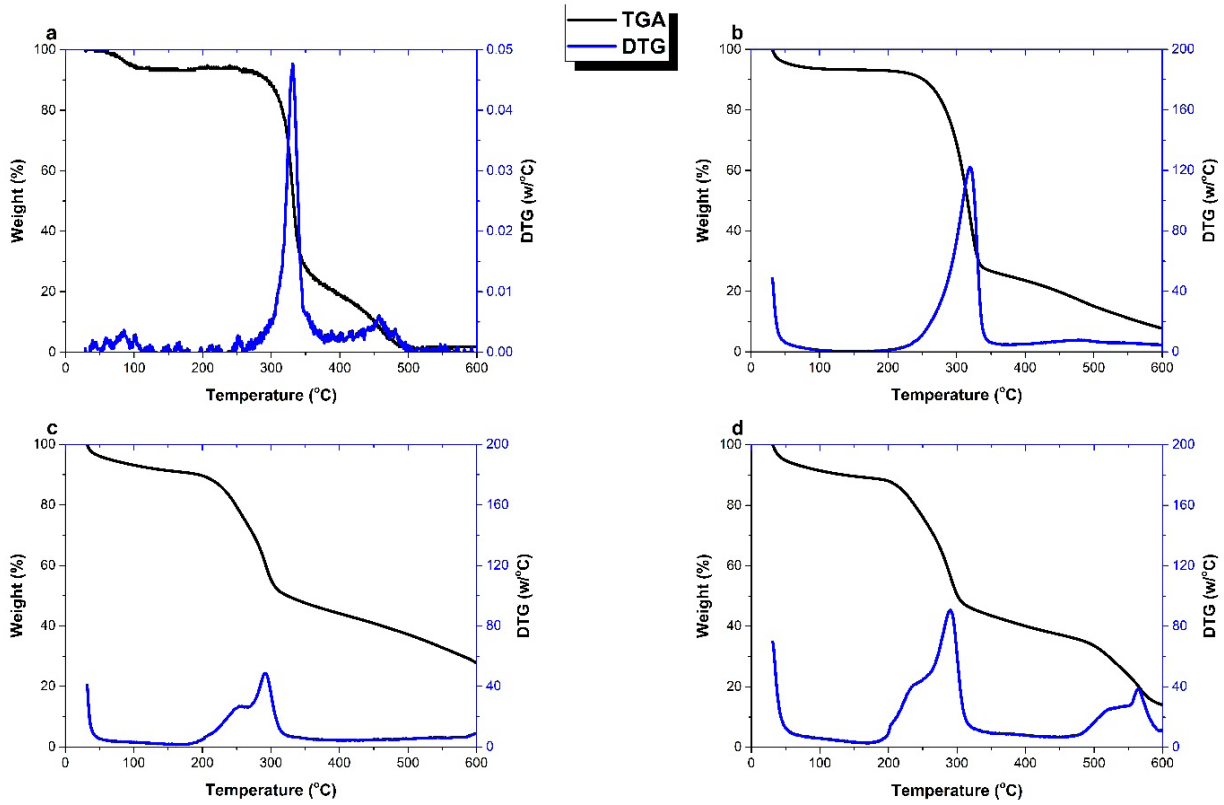

Figure 7: TGA and DTG curves of (a) α-cellulose, (b) CNF1, (c) CNF2 and (d) CNF3.

Table 3: Thermal analysis data of α-cellulose, CNF1, CNF2 and CNF3.

	Temperature of weight loss at specific mass					
Material	**$T_{10\%}$ (°C)**	**$T_{50\%}$ (°C)**	**T_{Onset} (°C)**	**T_{Max} (°C)**	**Residue (%)**	**CI (%)**
Cellulose	293.67	332.16	276.95	331.00	2.31	73.69
CNF1	251.62	315.89	235.81	320.85	7.76	73.45
CNF2	194.70	323.75	139.03	292.02	27.75	43.61
CNF3	136.25	301.01	126.04	291.02	13.84	55.26

The TGA data of all cellulosic materials can be used to determine the thermal stability and the degradation temperature of each sample (α-cellulose, CNF1, CNF2 and CNF3). The thermogravimetric and derivative thermogravimetric analysis of those cellulosic materials are shown in Figure 7.

The pyrolysis process is one process that can occur during the thermos-degradation process. Table 3 shows that the α-cellulose decomposed at the range of 276-331°C, but the decomposition temperature of CNF1 was slightly lower at 235-320°C. This lower value could be an implication of the smaller dimension of CNF1 fiber than α-cellulose fiber. The smaller dimension of fiber leads to the improvement of a specific surface area [36]. The lower thermal stability of CNF1 than α-cellulose is also caused by the surface modification of α-cellulose through the TEMPO oxidation, specifically it was suggested by the presence of the decarboxylation step as a result of the TEMPO-mediated oxidation. In the previous work of Fukuzumi et al, [25] the nanofibril cellulose was obtained from different sources, but had a similar carboxyl content which started to degrade at a similar temperature. Also, due to the chemical treatment using TEMPO, there is a possibility that the decrease of the degree of polymerization had an

Brought to you by | Universitat de Girona
Authenticated
Download Date | 1/31/20 2:37 PM

impact due to the decrease in the molecular weight of lignocellulose nanofiber leading to the decomposition process in the lower temperature [37].

From the CNF2 and CNF3 thermal analysis, the onset temperature occurred at 139 and 126°C, which is much lower than for the CNF1 and α-cellulose. Table 3 shows that the thermal stability of CNF1 is better than CNF2 and CNF3. This aligns with the explanation of other previous results [36,38–41]. The phenomenon that occurred on CNF1 is the impact of the oxidation reaction by TEMPO [25,41–43], but the phenomenon of CNF2 and CNF3 is caused by the lignin contamination [44]. The presence of lignin was supported by the lower value of the crystallinity index, especially of CNF2 and CNF3. Lignin and hemicellulose are called non-cellulosic amorphous polysaccharide which degrade at lower temperatures than the fiber which has a high crystallinity index.

To support the influence of lignocellulosic material in CNF, TGA analysis of lignin from other reports showed two steps of degradation. The first degradation occurred at around 100°C that attributed to water evaporation. The second step was the decomposition of hemicellulose and cellulose that occurred between 200°C and 400°C [39,45], respectively. The presence of lignin in CNF2 and CNF3 caused the reduction of the thermal stability. This statement can be used to explain the lower value of the degradation temperature of CNF2 and CNF3 compared to CNF1 and α-cellulose. The presence of lignin and hemicellulose in the fiber is one factor that influences the thermal stability of fiber. Based on the onset temperature value of CNF2 and CNF3, the lignin content plays a role to make the LCNF more thermally stable. It is due to the covalent linkage between lignin and cellulose fiber. As in Figure 7, especially for CNF3, there is an additional peak at 563°C that indicates the decomposition temperature of cellulose and hemicellulose or the decomposition of char [46,47]. This statement is supported by Nair & Yan [48] and Espinosa et al. [49], due to the presence of aromatic group, carbon-carbon bonds, lignin has a wide range of decomposition temperatures between 240-600°C, and with very few occurring around 400-600°C referring to the decomposition of cellulose and hemicellulose.

The residual mass of CNF1 at 600°C is higher than α-cellulose, and the thermal stability of CNF1 is less stable than α-cellulose. The thermal stability of CNF1 has been explained in the previous paragraph. The dehydration process at low temperatures can influence the yield of char. This reaction will induce the decomposition to occur at low temperatures. Table 3 also shows that CNF2 and CNF3 degraded more over a large temperature range. This can be influenced by the presence of lignin and hemicellulose of those materials. The removal of lignin and hemicellulose can be observed from the TGA graph. For lignin removal, as depicted in literature, the amount of residual mass is in the range between 250-600°C. This decreases with the increasing number of bleaching level [50,51]. On the other hand, the hemicellulose removal can be observed through the disappearance of the shoulder at 275°C of DTG curves [52]. In the DTG curve of CNF2 and CNF3, a shoulder shape that is identical to hemicellulose could be found at around 240-275°C. The residual mass of CNF2 and CNF3 decreased with the increasing in bleaching level (CNF2 = 2x bleaching and CNF3 = 3x bleaching). These results indicated increasing the number of bleaching level could enhance the removal of lignin and hemicellulose in the fiber.

4 Conclusion

Cellulose nanofiber (CNF) has been isolated from LEFB by the TEMPO-oxidized method. The TEMPO-oxidized is performed in three kinds of fiber, notably (i) α-cellulose of LEFB, (ii) raw fiber of LEFB with 2x bleaching level and (iii) raw fiber of LEFB with 3x bleaching level. The FT-IR spectra of α-cellulose and all CNFs showed almost similar bands, especially in the CNF2 and CNF3 where there was a different signal that confirmed the presence of lignin and hemicellulose. Those components influenced the morphology and thermal properties of fibers. The morphology analysis of α-cellulose confirmed that α-cellulose showed curled and well-defined fibrils. The XRD analysis revealed the crystallinity index of CNF1 was higher than CNF2 and CNF3 due to the removal of lignin and hemicellulose. In other analyses using TEM, CNF1 consisted of a bundle of microfibrils; however, different results were obtained on CNF2 and CNF3. The CNF2 fiber was more individualized than CNF3, and it can be assumed that CNF2 has a higher content of hemicellulose than CNF3. The thermal analysis showed the thermal stability of CNF1 (235-320°C) was better than CNF2 (139-292°C) and CNF3 (126-291°C). The residual mass of CNF2 was higher than CNF1 and CNF3.

Acknowledgement: Author thanks the Indonesian Ministry of Research, Technology and Higher Education (KEMENRISTEKDIKTI) for the PMDSU scholarship program and the financial support to conduct the research internship through PKPI-PMDSU 2017.

Conflict of Interest: Authors declare no conflict of interest

Brought to you by | Universitat de Girona
Authenticated
Download Date | 1/31/20 2:37 PM

Reference

[1] BPS-Statistic Indonesia. Indonesia Oil Palm Statistic 2016. Jakarta: 2017.

[2] Li W., Yue J., Liu S. Preparation of nanocrystalline cellulose via ultrasound and its reinforcement capability for poly(vinyl alcohol) composites, Ultrason. Sonochem., 2012, 19(3), 479–485. doi:10.1016/j.ultsonch.2011.11.007.

[3] Ghaderi M., Mousavi M., Yousefi H., Labbafi M. All-cellulose nanocomposite film made from bagasse cellulose nanofibers for food packaging application, Carbohyd. Polym., 2014, 104, 59–65. doi:10.1016/j.carbpol.2014.01.013.

[4] Eita M., Arwin H., Granberg H., Wågberg L. Addition of silica nanoparticles to tailor the mechanical properties of nanofibrillated cellulose thin films, J. Colloid Interf Sci., 2011, 363(2), 566–572. doi:10.1016/j.jcis.2011.07.085.

[5] Hu K., Kulkarni D.D., Choi I., Tsukruk V. V. Graphene-polymer nanocomposites for structural and functional applications, Prog. Polym. Sci., 2014, 39(11), 1934–1972. doi:10.1016/j.progpolymsci.2014.03.001.

[6] Ghazali A., Dermawan Y.M., Hafiz M.R., Zukeri M., Ibrahim R., Ghazali S. EFB nano fibrous cells for paper smoothing and improved printability, Adv. Mat. Res., 2014, 832, 537–542. doi:10.4028/www.scientific.net/AMR.832.537.

[7] Salajkova M., Valentini L., Zhou Q., Berglun L.A. Tough nanopaper structures based on cellulose nanofibers and carbon nanotubes, Compos. Sci. Technol., 2013, 87, 103–110. doi:10.1016/j.compscitech.2013.06.014.

[8] Qua E., Hornsby P., Sharma H., Lyons G. Preparation and characterisation of cellulose nanofibres, J. Mater. Sci., 2011, 46(18), 6029–6045. doi:10.1007/s10853-011-5565-x.

[9] Fatah I.Y.A., Abdul Khalil H.P.S., Hossain M.S., Aziz A.A., Davoudpour Y., Dungani R., et al. Exploration of a chemo-mechanical technique for the isolation of nanofibrillated cellulosic fiber from oil palm empty fruit bunch as a reinforcing agent in composites materials, Polymers-Basel., 2014, 6(10), 2611–2624. doi:10.3390/polym6102611.

[10] Saito T., Isogai A. Introduction of aldehyde groups on surfaces of native cellulose fibers by TEMPO-mediated oxidation, Colloids Surfaces A., 2006, 289(1–3), 219–225. doi:10.1016/j.colsurfa.2006.04.038.

[11] Saito T., Kimura S., Nishiyama Y., Isogai A. Cellulose Nanofibers Prepared by TEMPO-Mediated Oxidation of Native Cellulose, Biomacromolecules, 2007, 8(8), 2485–2491. doi:10.1021/bm0703970.

[12] González I., Boufi S., Pèlach M.A., Alcalà M., Vilaseca F., Mutjé P. Nanofibrillated cellulose as paper additive in eucalyptus pulps, BioResources, 2012, 7(4), 5167–5180. doi:10.15376/biores.7.4.5167-5180.

[13] Lee H.-R., Kim K., Mun S.C., Chang Y.K., Choi S.Q. A new method to produce cellulose nanofibrils from microalgae and the measurement of their mechanical strength, Carbohyd. Polym., 2018, 180, 276–285. doi:10.1016/j.carbpol.2017.09.104.

[14] Emami Z., Meng Q., Pircheraghi G., Manas-Zloczower I. Use of surfactants in cellulose nanowhisker/epoxy nanocomposites: effect on filler dispersion and system properties, Cellulose, 2015, 22(5), 3161–3176. doi:10.1007/s10570-015-0728-6.

[15] Jia Y., Zhai X., Fu W., Liu Y., Li F., Zhong C. Surfactant-free emulsions stabilized by tempo-oxidized bacterial cellulose, Carbohyd. Polym., 2016, 151, 907–915. doi:10.1016/j.carbpol.2016.05.099.

[16] Kuramae R., Saito T., Isogai A. TEMPO-oxidized cellulose nanofibrils prepared from various plant holocelluloses, React. Funct. Polym., 2014, 85, 126–133. doi:10.1016/j.reactfunctpolym.2014.06.011.

[17] Mahendra I.P., Wirjosentono B., Tamrin, Ismail H., Mendez J.A. Oil Palm-Based Nanocrystalline Cellulose in The Emulsion System of Cyclic Natural Rubber, Rasayan J. Chem., 2019, 12(2), 635–640. doi:10.31788/RJC.2019.1225089.

[18] Fahma F., Iwamoto S., Hori N., Iwata T., Takemura A. Isolation, preparation, and characterization of nanofibers from oil palm empty-fruit-bunch (OPEFB), Cellulose, 2010, 17(5), 977–985. doi:10.1007/s10570-010-9436-4.

[19] Jonoobi M., Harun J., Shakeri A., Misra M., Oksmand K. Chemical composition, crystallinity, and thermal degradation of bleached and unbleached kenaf bast (Hibiscus cannabinus) pulp and nanofibers, BioResources, 2009, 4(2), 626–639. doi:10.15376/biores.4.2.626-639.

[20] Saka S., Munusamy M.., Shibata M., Tono Y., Miyafuji H. Chemical Constituent of The Different Anatomical Parts of The Oil Palm (Elaeis guineensis) for Their Sustainable Utilization. Nat. Resour. Energy Environ., Kyoto: 2008, p. 19–34.

[21] Ohwoavworhua F.O., Adelakun T.A. Some Physical Characteristics of Microcrystalline Cellulose Obtained from Raw Cotton of Cochlospermum planchonii, Trop. J. Pharm. Res., 2007, 4(2), 501–507. doi:10.4314/tjpr.v4i2.14626.

[22] Segal L., Creely J.J., Martin A.E., Conrad C.M. An Empirical Method for Estimating the Degree of Crystallinity of Native Cellulose Using the X-Ray Diffractometer, Text. Res. J., 1959, 29(10), 786–794. doi:10.1177/004051755902901003.

[23] Ahuja D., Kaushik A., Singh M. Simultaneous extraction of lignin and cellulose nanofibrils from waste jute bags using one pot pre-treatment, Int. J. Biol. Macromol., 2018, 107, 1294–1301. doi:10.1016/j.ijbiomac.2017.09.107.

[24] Tanaka R., Saito T., Isogai A. Cellulose nanofibrils prepared from softwood cellulose by TEMPO/NaClO/NaClO2 systems in water at pH 4.8 or 6.8, Int. J. Biol. Macromol., 2012, 51(3), 228–234. doi:10.1016/j.ijbiomac.2012.05.016.

[25] Fukuzumi H., Saito T., Okita Y., Isogai A. Thermal stabilization of TEMPO-oxidized cellulose, Polym. Degrad. Stabil., 2010, 95(9), 1502–1508. doi:10.1016/j.polymdegradstab.2010.06.015.

[26] Jaušovec D., Vogrinčič R., Kokol V. Introduction of aldehyde vs. carboxylic groups to cellulose nanofibers using laccase/TEMPO mediated oxidation, Carbohyd. Polym., 2015, 116, 74–85. doi:10.1016/j.carbpol.2014.03.014.

[27] Coseri S., Biliuta G., Simionescu B.C., Stana-Kleinschek K., Ribitsch V., Harabagiu V. Oxidized cellulose—Survey of the most recent achievements, Carbohyd. Polym., 2013, 93(1), 207–215. doi:10.1016/j.carbpol.2012.03.086.

[28] Gamelas J.A.F.F., Pedrosa J., Lourenço A.F., Mutjé P., González I., Chinga-Carrasco G., et al. On the morphology of cellulose nanofibrils obtained by TEMPO-mediated oxidation and mechanical treatment, Micron, 2015, 72, 28–33. doi:10.1016/j.micron.2015.02.003.

[29] Besbes I., Alila S., Boufi S. Nanofibrillated cellulose from TEMPO-oxidized eucalyptus fibres: Effect of the carboxyl

Brought to you by | Universitat de Girona
Authenticated
Download Date | 1/31/20 2:37 PM

content, Carbohyd. Polym., 2011, 84(3), 975–983. doi:10.1016/j.carbpol.2010.12.052.
[30] Ching Y.C., Ng T.S. Effect of preparation conditions on cellulose from oil palm empty fruit bunch fiber, BioResources, 2014, 9(4), 6373–6385. doi:10.15376/biores.9.4.6373-6385.
[31] Chaker A., Alila S., Mutjé P., Vilar M.R., Boufi S. Key role of the hemicellulose content and the cell morphology on the nanofibrillation effectiveness of cellulose pulps, Cellulose, 2013, 20(6), 2863–2875. doi:10.1007/s10570-013-0036-y.
[32] Delgado-Aguilar M., González I., Tarrés Q., Pèlach M.À., Alcalà M., Mutjé P. The key role of lignin in the production of low-cost lignocellulosic nanofibres for papermaking applications, Ind. Crop. Prod., 2016, 86, 295–300. doi:10.1016/j.indcrop.2016.04.010.
[33] Qing Y., Cai Z., Wu Y., Yao C., Wu Q., Li X. Facile preparation of optically transparent and hydrophobic cellulose nanofibril composite films, Ind. Crop. Prod., 2015, 77, 13–20. doi:10.1016/j.indcrop.2015.08.016.
[34] Rohaizu R., Wanrosli W.D. Sono-assisted TEMPO oxidation of oil palm lignocellulosic biomass for isolation of nanocrystalline cellulose, Ultrason. Sonochem., 2017, 34, 631–639. doi:10.1016/j.ultsonch.2016.06.040.
[35] Okita Y., Saito T., Isogai A. Entire Surface Oxidation of Various Cellulose Microfibrils by TEMPO-Mediated Oxidation, Biomacromolecules, 2010, 11(6), 1696–1700. doi:10.1021/bm100214b.
[36] Sofla M.R.K., Brown R.J., Tsuzuki T., Rainey T.J. A comparison of cellulose nanocrystals and cellulose nanofibres extracted from bagasse using acid and ball milling methods, Adv. Nat. Sci-Nanosci., 2016, 7(3). doi:10.1088/2043-6262/7/3/035004.
[37] Isogai A., Saito T., Fukuzumi H. TEMPO-oxidized cellulose nanofibers, Nanoscale, 2011, 3(1), 71–85. doi:10.1039/c0nr00583e.
[38] Rosa M.F., Medeiros E.S., Malmonge J.A., Gregorski K.S., Wood D.F., Mattoso L.H.C., et al. Cellulose nanowhiskers from coconut husk fibers: Effect of preparation conditions on their thermal and morphological behavior, Carbohyd. Polym., 2010, 81(1), 83–92. doi:10.1016/j.carbpol.2010.01.059.
[39] Horseman T., Tajvidi M., Diop C.I.K., Gardner D.J. Preparation and property assessment of neat lignocellulose nanofibrils (LCNF) and their composite films, Cellulose, 2017, 24(6), 2455–2468. doi:10.1007/s10570-017-1266-1.
[40] Jiang F., Hsieh Y.-L. Chemically and mechanically isolated nanocellulose and their self-assembled structures, Carbohyd. Polym., 2013, 95(1), 32–40. doi:10.1016/j.carbpol.2013.02.022.
[41] Du C., Li H., Li B., Liu M., Zhan H. Characteristics and properties of cellulose nanofibers prepared by TEMPO oxidation of corn husk, BioResources, 2016, 11(2), 5276–5284. doi:10.15376/biores.11.2.5276-5284.
[42] Shen D.K., Gu S. The mechanism for thermal decomposition of cellulose and its main products, Bioresource Technol., 2009, 100(24), 6496–6504. doi:10.1016/j.biortech.2009.06.095.
[43] Deepa B., Abraham E., Cordeiro N., Mozetic M., Mathew A.P., Oksman K., et al. Utilization of various lignocellulosic biomass for the production of nanocellulose: a comparative study, Cellulose, 2015, 22(2), 1075–1090. doi:10.1007/s10570-015-0554-x.
[44] Feng Y.H., Cheng T.Y., Yang W.G., Ma P.T., He H.Z., Yin X.C., et al. Characteristics and environmentally friendly extraction of cellulose nanofibrils from sugarcane bagasse, Ind. Crop. Prod., 2018, 111, 285–291. doi:10.1016/j.indcrop.2017.10.041.
[45] Yang H., Yan R., Chen H., Lee D.H., Zheng C. Characteristics of hemicellulose, cellulose and lignin pyrolysis, Fuel, 2007, 86(12–13), 1781–1788. doi:10.1016/j.fuel.2006.12.013.
[46] Jain R.K., Lal K., Bhatnagar H.L. Thermal studies on C-6 substituted cellulose and its subsequent C-2 and C-3 esterified products in air, Eur. Polym. J., 1986, 22(12), 993–1000. doi:10.1016/0014-3057(86)90081-9.
[47] Aggarwal P., Dollimore D. The combustion of starch, cellulose and cationically modified products of these compounds investigated using thermal analysis, Thermochim. Acta, 1997, 291(1–2), 65–72. doi:10.1016/s0040-6031(96)03103-6.
[48] Nair S.S., Yan N. Effect of high residual lignin on the thermal stability of nanofibrils and its enhanced mechanical performance in aqueous environments, Cellulose, 2015, 22(5), 3137–3150. doi:10.1007/s10570-015-0737-5.
[49] Espinosa E., Sánchez R., González Z., Domínguez-Robles J., Ferrari B., Rodríguez A. Rapidly growing vegetables as new sources for lignocellulose nanofibre isolation: Physicochemical, thermal and rheological characterisation, Carbohyd. Polym., 2017, 175, 27–37. doi:10.1016/j.carbpol.2017.07.055.
[50] Chirayil C.J., Joy J., Mathew L., Mozetic M., Koetz J., Thomas S. Isolation and characterization of cellulose nanofibrils from Helicteres isora plant, Ind. Crop. Prod., 2014, 59, 27–34. doi:10.1016/j.indcrop.2014.04.020.
[51] Xie J., Hse C.-Y., De Hoop C.F., Hu T., Qi J., Shupe T.F. Isolation and characterization of cellulose nanofibers from bamboo using microwave liquefaction combined with chemical treatment and ultrasonication, Carbohyd. Polym., 2016, 151, 725–734. doi:10.1016/j.carbpol.2016.06.011.
[52] Kabir M.M., Wang H., Lau K.T., Cardona F. Effects of chemical treatments on hemp fibre structure, Appl. Surf. Sci., 2013, 276, 13–23. doi:10.1016/j.apsusc.2013.02.086.

Brought to you by | Universitat de Girona
Authenticated
Download Date | 1/31/20 2:37 PM